JOURNAL OF APPLIED PHYSICS VOLUME 96, NUMBER 4 15 AUGUST 2004

Hybrid techniques for electrostatic analysis of nanoelectromechanical systems

Gang Li and N. R. Aluru[a)]
Beckman Institute for Advanced Science and Technology, University of Illinois at Urbana-Champaign, Urbana, Illinois 61801

(Received 19 March 2004; accepted 17 May 2004)

In this paper, we propose an efficient approach, namely the hybrid BIE/Poisson/Schrödinger approach, for electrostatic analysis of nanoelectromechanical systems. In this approach, the interior and the exterior domain electrostatics are described by Poisson's equation (or Poisson's equation coupled with Schrödinger's equation when quantum-mechanical effects are dominant) and the boundary integral formulation (BIE) of the potential equation, respectively. We employ a meshless finite cloud method and a boundary cloud method to solve the coupled BIE/Poisson/Schrödinger's equations self-consistently. The proposed approach significantly reduces the computational cost and provides a higher accuracy of the solution. © *2004 American Institute of Physics*.
[DOI: 10.1063/1.1769608]

I. INTRODUCTION

A number of nanoelectromechanical device and system (NEMS) applications have been proposed recently.[1] These applications range from molecular memory, computing, low-power switches, actuators, and a variety of chemical, mechanical, and biological sensors. Even though a variety of forces can be used to actuate nanostructures, electrostatic potentials are gaining a lot of interest because of some advantages in nanostructure fabrication and control. As the size of the mechanical component (typically a semiconductor material, such as silicon) continues to shrink to nanoscale and subnanoscales, quantum effects become more significant and can even dominate the entire device behavior. The carrier quantum confinement in the semiconductor structure can impose a significant effect on the charge distribution in the mechanical components of NEMS. As a result, classical electrostatic analysis is inaccurate at nanoscales. For nanometer scale semiconductor devices, coupled Poisson/Schrödinger equations need to be solved self-consistently to obtain the electronic properties such as the potential field and the charge distribution of the system.[2–6] However, in contrast to classical semiconductor devices (e.g., MOSFETs), NEMS typically contain structures with complex geometries and configurations. The electrostatic analysis of NEMS must include both the exterior and the interior regions of the NEM structures—this is referred to as an open boundary problem. Conventionally, to solve such an open boundary problem, a spatial region (cutoff box)[7–12] covering the system of interest is selected such that the potential variation outside the region has little influence on the system. The region is then discretized into elements or points depending on the numerical method used. An issue with the conventional approach is that the equations need to be solved over a quite large area of the dielectric medium while only the electronic properties within the semiconductor are of interest. For this reason, solving Poisson's and Schrödinger's equations over the entire cutoff box is quite inefficient and very expensive.

Boundary integral formulations and boundary element methods (BEM)[13] are attractive computational techniques for linear and exterior problems as they reduce the dimensionality of the original problem. For example, for three-dimensional (3D) problems, the boundary element method requires discretization of the two-dimensional surface of the 3D object and for 2D problems, the boundary element method requires discretization of the one-dimensional boundary. For exterior problems, the use of classical methods, such as the finite difference (FDM),[14] or the finite element method (FEM),[15] requires discretization of the entire exterior, whereas with a boundary element method only the surface needs to be discretized. For this reason, the boundary integral formulations are advantageous for exterior electrostatic analysis. The boundary integral equations (BIEs) for exterior electrostatic analysis have been proposed in the literature.[16,17] A coupled FEM/BEM approach for electrostatic analysis of semiconductor MOSFETs has been proposed in Ref. 18. However, in Ref. 18, an artifical boundary (cutoff box) is still constructed and discretized in the dielectric medium. Since multiple large surface areas of NEMS structures can be exposed to the dielectric medium, the construction of artificial boundaries for NEMS structures could be awkward.

In this paper, we propose an approach, referred to as the hybrid BIE/Poisson/Schrödinger approach, for electrostatic analysis of NEMS. The key idea in this approach is to solve Laplace's equation in the exterior domain of the NEM structures using a boundary integral formulation, and then to combine the BIEs with Poisson's equation or Poisson/Schrödinger equations for the interior domain analysis of the semiconductor structures. The BIEs are defined only on the surface of the semiconductors/conductors with no artificial boundaries. We employ meshless numerical methods, namely the finite cloud method for interior analysis (i.e., for

[a)]Author to whom correspondence should be addressed; present address: Department of Mechanical & Industrial Engineering, UIUC; electronic mail: aluru@uiuc.edu, URL: http://www.uiuc.edu/~aluru

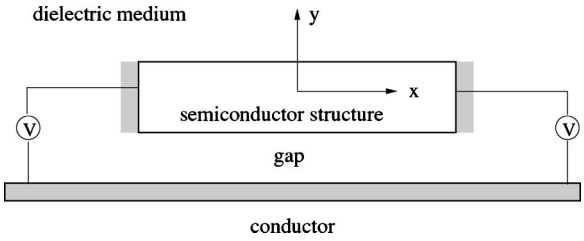

FIG. 1. A typical nanoswitch consisting of a fixed-fixed semiconductor and a bottom conductor.

the solution of Poisson's equation or Poisson/Schrödinger equations in the semiconductor) and the boundary cloud method for exterior analysis (i.e., for the solution of the boundary integral equations of the exterior potential equation). The potential and the charge distributions are obtained by solving the coupled system of equations self-consistently. It is shown in the paper that the proposed approach is more efficient and more accurate compared to the conventional cutoff box approach.

The rest of the paper is organized as follows: Sec. II introduces the electrostatic analysis of NEMS, Sec. III presents the BIEs for semiconductors, Sec. IV describes the hybrid BIE/Poisson approach, Sec. V describes the hybrid BIE/Poisson/Schrödinger approach, Sec. VI presents numerical results, and Sec. VII presents conclusions.

II. ELECTROSTATIC ANALYSIS OF NANOELECTROMECHANICAL SYSTEMS (NEMS)

To illustrate the electrostatic analysis of NEMS, we consider a nanoswitch example as shown in Fig. 1. The nanoswitch consists of a semiconductor beam structure that is clamped at the ends and the beam is separated from a bottom conductor/electrode by a small gap. When a voltage is applied between the fixed-fixed beam and the bottom conductor, electrostatic charges are induced in the semiconductor beam. These charges give rise to an electrostatic force, which acts on the entire (surface as well as the interior) semiconductor beam. Since the bottom conductor is fixed and can not move, the electrostatic forces deform the fixed-fixed beam. In this paper, we focus on the electrostatics analysis of NEMS, i.e., we would like to compute the electrostatic charge distribution in the semiconductor NEM structures.

The nanoswitch shown in Fig. 1 contains three regions: the semiconductor structure, the bottom conductor, and the infinite dielectric medium. The bottom conductor region is treated as an equipotential region. Based on the idealization that the dielectric medium is a perfect insulator, i.e., there is no charge in the entire dielectric medium, the electric potential satisfies the Laplace equation in the dielectric medium (the region exterior to the semiconductor and the conductor structures). When the critical length (e.g., the width) of the semiconductor structure is comparable to the Debye length or the screening length,[19] the potential inside the semiconductor satisfies Poisson's equation. As the size of the semiconductor structure continues to shrink to nanoscale and subnanoscales, quantum effects become more significant and can even dominate the entire device behavior.[20] The carrier quantum confinement in the semiconductor structure can impose a significant effect on the charge distribution in the mechanical components of NEMS. In this case, Poisson/Schrödinger equations need to be solved self-consistently on the semiconductor structure to obtain the potential field and the charge distribution.

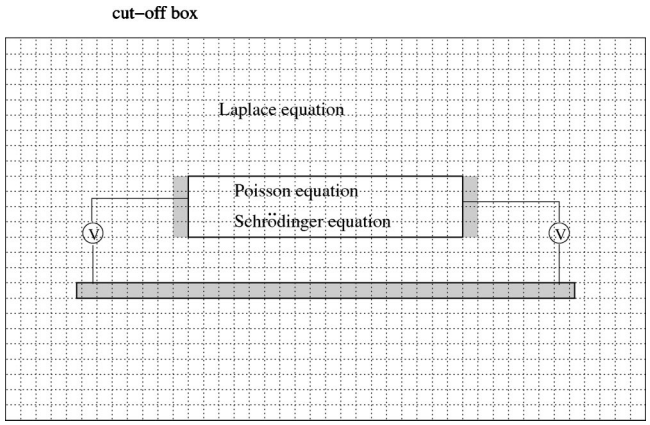

FIG. 2. Typical domain discretization for electrostatic analysis of the nanoswitch shown in Fig. 1.

In typical semiconductor MOSFET simulations, an approximated Dirichlet, Neumann, or impedance-type boundary condition[3,21–23] can be applied at the dielectric medium/semiconductor interface to avoid discretizing the exterior domain. However, in NEMS applications, the approximated boundary conditions are not valid since a large portion of the semiconductor structure is exposed to the dielectric medium, the gap between the semiconductor structures and the electrodes can be large and NEM structures can be complex. Alternatively, to solve the Laplace/Poisson/Schrödinger equations, one can adopt the conventional approach, in which a spatial region (cutoff box) covering the system of interest is selected such that the potential variation outside the region has little influence on the system. The region is then discretized into elements or points depending on the numerical method used. Figure 2 shows a typical discretization of the nanoswitch shown in Fig. 1. Potential boundary conditions are prescribed on the bottom conductor and at the ends of the fixed-fixed semiconductor beam. Based on the assumption that the potential variation outside the cutoff box is negligible, a zero electric field normal to the boundary is applied as the boundary condition at the outer boundary of the cutoff box. The next step is to use a numerical method (typically a finite difference or a finite element method) to solve for the potential in the entire discretized region. After the potential is obtained, the charge distribution in the NEM structure can be computed. Although the conventional approach is straightforward, it has several disadvantages.

(1) The cutoff box is an approximation and the definition of the cutoff box needs a good judgment. Inaccurate results could be obtained if the cutoff box is too small. However, computational cost could be very high if the cutoff box is too large.

(2) The entire spatial region needs to be discretized even if the cutoff box is properly chosen. For this reason, the system has many degrees of freedom (DOF), which means a

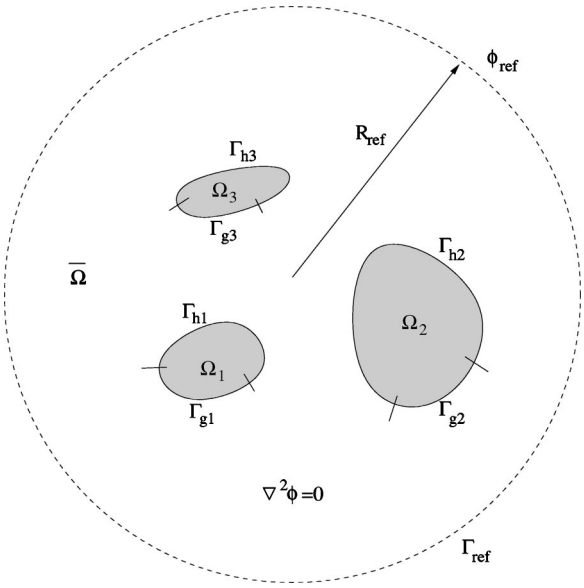

FIG. 3. A system of semiconductors.

large nonlinear system needs to be solved numerically. Furthermore, the DOF scale as $O(N^3)$ in 3D where N is the number of points/elements in a single dimension. Computational cost is a major issue in this approach.

In this paper, we propose a hybrid technique to solve the open boundary problem efficiently. The key idea is to employ a boundary integral formulation, which is defined only on the boundary of the NEM structures, for the exterior electrostatic analysis, and to solve the coupled BIE/Poisson/Schrödinger equations self-consistently. The proposed technique is referred to as the hybrid BIE/Poisson/Schrödinger approach.

III. BOUNDARY INTEGRAL EQUATIONS FOR SEMICONDUCTORS

We will deal with two-dimensional electrostatic problems in this paper, but the approach can be extended easily for three-dimensional problems. Consider a system of objects including semiconductors and conductors $(\Omega_1, \Omega_2, \ldots, \Omega_{N_o})$, where N_o is the number of objects, embedded in a uniform dielectric medium $\overline{\Omega}$ as shown in Fig. 3, potential $g_i(\mathbf{x})$, $i=1,2,\ldots,N_o$, and the normal derivative of the potential $h_i(\mathbf{x})$, $i=1,2,\ldots,N_o$ are applied on certain portions of the boundary of each semiconductor, Γ_{gi} and Γ_{hi}, $i=1,2,\ldots,N_o$, respectively. The potential field in the dielectric medium $\overline{\Omega}$ can be determined by the potential theory. The governing equation along with the boundary conditions for the exterior electrostatic problem are given by [24]

$$\nabla^2\phi = 0 \quad \text{in } \overline{\Omega} \tag{1}$$

$$\phi = g_i(\mathbf{x}) \quad \text{on } \Gamma_{gi} \quad i=1,2,\ldots,N_o, \tag{2}$$

$$q = \frac{\partial\phi}{\partial n} = h_i(\mathbf{x}) \quad \text{on } \Gamma_{hi} \quad i=1,2,\ldots,N_o, \tag{3}$$

where $\mathbf{x}=\{x,y\}$ is the position vector of a point, $g_i(\mathbf{x})$ and $h_i(\mathbf{x})$ are the potential and its normal derivative specified on the boundary portions Γ_{gi} and Γ_{hi} of the semiconductor i, $i=1,2,\ldots,N_o$, respectively. Note that the exterior domain $\overline{\Omega}$ is an open domain. Typically, a reference potential ϕ_{ref} needs to be specified on a reference plane Γ_{ref} far away from the conductors. For a 2D system, as shown in Fig. 3, a circular reference plane can be used, i.e.,

$$\phi = \phi_{ref} \quad \text{on } \Gamma_{ref} \tag{4}$$

Note that ϕ_{ref} becomes the reference potential ϕ_∞ when the radius of the reference plane $R_{ref}\to\infty$.

An efficient approach to treat the exterior electrostatic problem given in Eqs. (1)–(4) is to use the boundary integral formulation. Boundary integral formulations for exterior electrostatic analysis have been well developed and published in the literature (see, e.g., Refs. 16 and 12 for an overview). In this section, we derive the boundary integral equations for a system containing multiple semiconductors by using some results given in Refs. 16 and 17.

The boundary integral equation for a general exterior potential problem is given by Ref. 13,

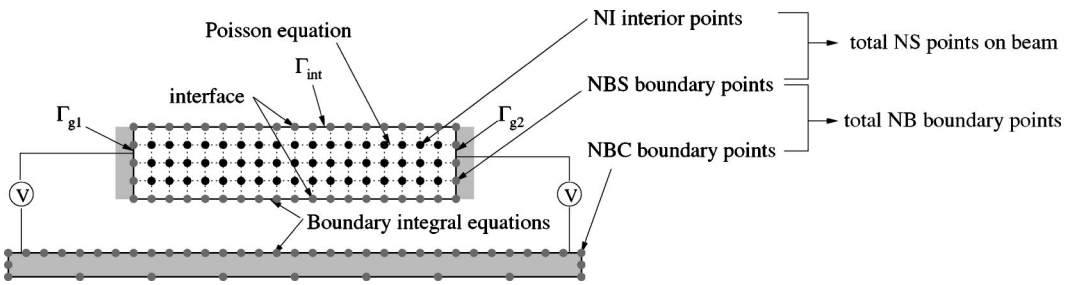

FIG. 4. Hybrid BIE/Poisson discretization of the domain. There are *NS* points on the semiconductor beam which include *NI* interior points and *NBS* boundary points. There are also *NBC* points on the boundary of the bottom conductor. Therefore, the total number of points on the boundary of the structures, including the semiconductor beam and the bottom conductor, is *NBS*+*NBC*=*NB*. Note that no exterior discretization is necessary.

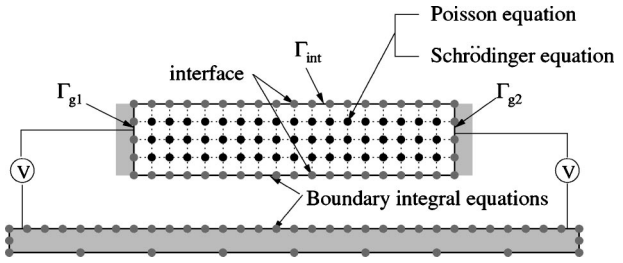

FIG. 5. Hybrid BIE/Poisson/Schrödinger discretization of the nanoswitch domain.

$$\alpha(\mathbf{x})\phi(\mathbf{x}) = \sum_{j=1}^{N_o} \int_{\Gamma_j} \phi(\mathbf{x}') \frac{\partial G(\mathbf{x},\mathbf{x}')}{\partial n'} d\Gamma(\mathbf{x}') + \phi_{ref} \int_{\Gamma_{ref}} \frac{\partial G(\mathbf{x},\mathbf{x}')}{\partial n'} d\Gamma(\mathbf{x}') - \sum_{j=1}^{N_o} \int_{\Gamma_j} q(\mathbf{x}') G(\mathbf{x},\mathbf{x}') d\Gamma(\mathbf{x}') - \int_{\Gamma_{ref}} q(\mathbf{x}') G(\mathbf{x},\mathbf{x}') d\Gamma(\mathbf{x}'), \tag{5}$$

where $\mathbf{x}$ is the source point, $\mathbf{x}'$ is the field point, $G(\mathbf{x},\mathbf{x}')$ is the Green's function, n' is the outward normal at $\mathbf{x}'$, $q(\mathbf{x}') = \partial\phi(\mathbf{x}')/\partial n'$ is the flux at the field point $\mathbf{x}'$, $\alpha(\mathbf{x})$ is the corner tensor [$\alpha(\mathbf{x}) = 1/2$ for smooth boundaries, see Ref. 13 for more details] and $\Gamma_j = \Gamma_{gj} \cup \Gamma_{hj}$. In two-dimensions, $G(\mathbf{x},\mathbf{x}') = \ln|\mathbf{x}-\mathbf{x}'|/(2\pi)$, where $|\mathbf{x}-\mathbf{x}'|$ is the distance between the source point $\mathbf{x}$ and the field point $\mathbf{x}'$. It can be shown that when the source point is on a semiconductor j, i.e., $\mathbf{x} \in \Gamma_j$, $j = 1,2,\ldots,N_o$, the second term on the right-hand side of Eq. (5) can be rewritten as[16]

$$\phi_{ref} \int_{\Gamma_{ref}} \frac{\partial G(\mathbf{x},\mathbf{x}')}{\partial n'} d\Gamma(\mathbf{x}') = \phi_{ref} \times 1 = \phi_{ref}. \tag{6}$$

When the radius of the reference plane goes to the infinity, $R_{ref} \to \infty$, the reference plane Γ_{ref} goes to Γ_∞ and the Green's function $G(\mathbf{x},\mathbf{x}') \to G_\infty$. Since G_∞ is a constant for any field point $\mathbf{x}' \in \Gamma_j$, $j = 1,2,\ldots,N_o$, the fourth term on the right-hand side of Eq. (5) becomes

$$\lim_{R_{ref}\to\infty} \int_{\Gamma_{ref}} q(\mathbf{x}') G(\mathbf{x},\mathbf{x}') d\Gamma(\mathbf{x}') = G(\infty) \int_{\Gamma_\infty} q(\mathbf{x}') d\Gamma(\mathbf{x}'). \tag{7}$$

Assuming the variation of the potential vanishes, i.e., $q(\mathbf{x}') = 0$ on Γ_∞, it can be shown that[16]

$$\sum_{j=1}^{N_o} \int_{\Gamma_j} q(\mathbf{x}') d\Gamma(\mathbf{x}') = 0. \tag{8}$$

Substituting Eqs. (6)–(8) into Eq. (5), one obtains

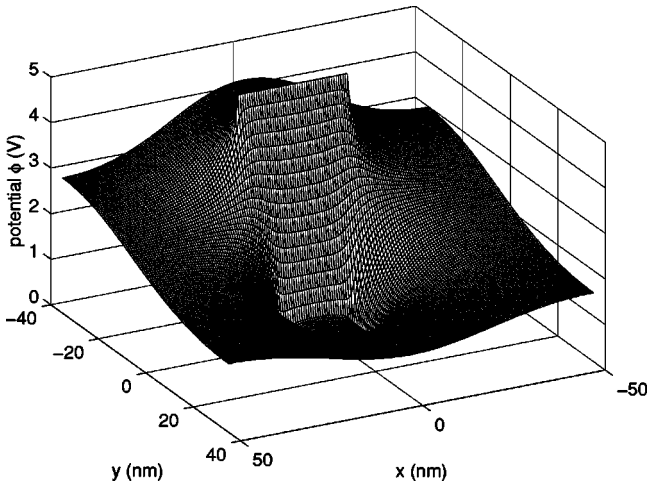

FIG. 6. Potential profile obtained by using the conventional cutoff box approach.

$$\alpha(\mathbf{x})\phi(\mathbf{x}) = \sum_{j=1}^{N_o} \int_{\Gamma_j} \phi(\mathbf{x}') \frac{\partial G(\mathbf{x},\mathbf{x}')}{\partial n'} d\Gamma(\mathbf{x}') - \sum_{j=1}^{N_o} \int_{\Gamma_j} q(\mathbf{x}') G(\mathbf{x},\mathbf{x}') d\Gamma(\mathbf{x}') + \phi_\infty, \tag{9}$$

where ϕ_∞ is the constant reference potential on Γ_∞. Equations (8) and (9) are the boundary integral equations for exterior electrostatic analysis of semiconductors.

IV. HYBRID BIE/POISSON APPROACH FOR SEMICLASSICAL ELECTROSTATIC ANALYSIS

Since the quantities in Eqs. (8) and (9) are defined only on the boundary of the semiconductors or conductors, using the boundary integral equations for the exterior domain eliminates the need to discretize the region exterior to the NEM structures and the requirement of a cutoff box. For the interior domain of the semiconductor structure, the electric potential typically satisfies Poisson's equation. The governing equations in the semiclassical model are given by[19]

$$\nabla \cdot (\varepsilon_s \nabla \phi) = -e(p - n + N_D^+ - N_A^-), \tag{10}$$

where e is the elementary charge, ε_s is the permittivity of the semiconductor material, N_D^+ and N_A^- are the density of ionized donor and acceptor dopants, respectively, and p and n are the hole and electron concentrations given by

$$p(\phi) = 2\left(\frac{m_p^* k_B T}{2\pi\hbar^2}\right)^{3/2} \mathcal{F}_{1/2}\left(\frac{E_V - E_F}{k_B T}\right), \tag{11}$$

$$n(\phi) = 2\left(\frac{m_n^* k_B T}{2\pi\hbar^2}\right)^{3/2} \mathcal{F}_{1/2}\left(\frac{E_F - E_C}{k_B T}\right), \tag{12}$$

where E_F is the Fermi level energy, $\hbar$ is Planck's constant, k_B is the Boltzmann constant, T is the temperature, $\mathcal{F}_{1/2}$ is the complete Fermi-Dirac integral of order $1/2$, E_C and E_V are the conduction/valence band energy, respectively, and m_n^* and m_p^* are the density-of-state masses of the conduction and the valence band, respectively. Combining the boundary integral equations [Eqs. (8) and (9)] for the exterior domain and Pois-

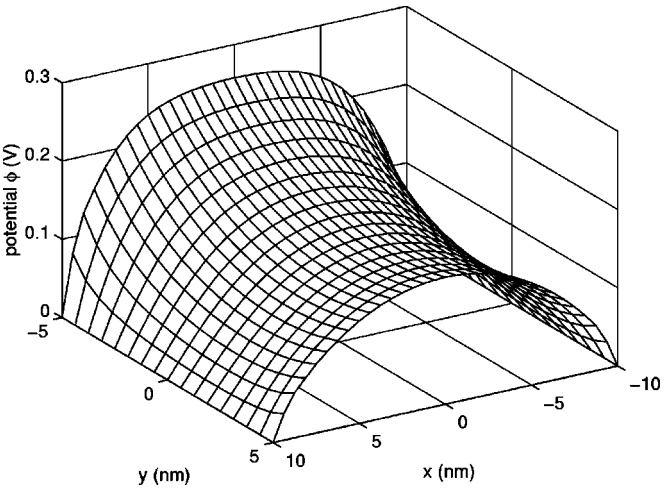

FIG. 7. Potential profile obtained from the hybrid BIE/Poisson approach.

son's equation [Eq. (10)] for the interior domain of the semiconductor structures, we propose a hybrid BIE/Poisson approach for semiclassical electrostatic analysis. Figure 4 shows the domain discretization scheme of the nanoswitch by using the hybrid approach. The fixed-fixed semiconductor beam and the boundary of the bottom conductor are represented by a set of nodes. In the hybrid approach, we enforce that the boundary integral equations are satisfied at the boundary nodes and Poisson's equation is satisfied at the interior nodes of the semiconductor beam. Schottky contacts are applied at the two ends of the semiconductor beam and the potential is known, i.e.,

$$\phi = g \quad \text{on } \Gamma_{g1} \text{ and } \Gamma_{g2} \tag{13}$$

At the interface between the semiconductor beam and the dielectric medium, the boundary integral equation and Poisson's equation are coupled by the interface conditions[24]

$$\phi|_{BIE} = \phi|_{Poisson} \quad \text{on } \Gamma_{int}, \tag{14}$$

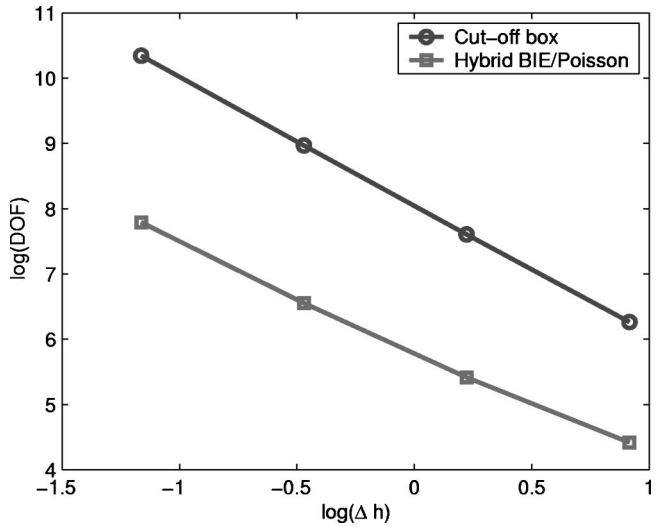

FIG. 8. Degree of freedom comparison between the Poisson and the hybrid BIE/Poisson approaches (Δh is the point spacing).

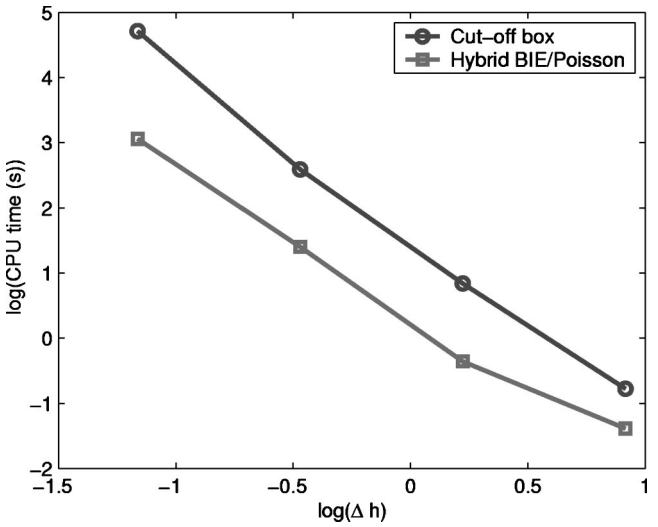

FIG. 9. CPU time comparison between the Poisson and the hybrid BIE/Poisson approaches.

$$\varepsilon_s q|_{Poisson} + \varepsilon_d q|_{BIE} = \sigma \quad \text{on } \Gamma_{int}, \tag{15}$$

where $\phi|_{BIE}$ and $\phi|_{Poisson}$ are the potentials from the boundary integral equation and Poisson's equation, respectively, $q|_{BIE}$ and $q|_{Poisson}$ are the normal derivatives of the potential from the boundary integral equation and Poisson's equation, respectively, ε_d is the permittivity of the dielectric medium, and σ is the charge density on the exposed surface of the semiconductor. In this paper, for the purpose of illustration of the hybrid approach, the charge density on the surface is assumed to be zero. However, other models for the interface charge density σ can also be implemented.

In the hybrid BIE/Poisson approach, we employ a finite cloud method (FCM) (Refs. 25–27) for solving Poisson's equation [Eq. (10)] at the interior nodes of the semiconductor beam and a boundary cloud method (BCM) (Refs. 28 and 29) for solving the boundary integral equations given in Eqs.

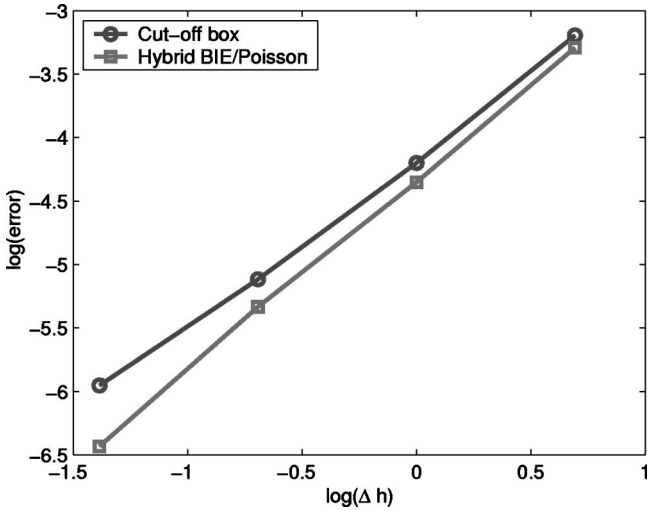

FIG. 10. Convergence comparison between the Poisson and the hybrid BIE/Poisson approaches (Δh is the point spacing). The error is defined by $\text{error} = 1/(|\phi|^{ref}_{\max})\sqrt{(1/NS)\sum_{i=1}^{NS}[\phi^{ref}(\mathbf{x}_i) - \phi^a(\mathbf{x}_i)]^2}$, where ϕ^{ref} is the reference solution obtained by using a fine point distribution and ϕ^a is the computed solution obtained from the coarser point distributions.

(8) and (9) at the boundary nodes. The finite cloud method is a true meshless method (see Ref. 30 for an overview of meshless methods) in which only points are needed to cover the structural domain and no connectivity information among the points is required. The finite cloud method uses a fixed kernel technique to construct the approximation functions and a point collocation technique to discretize the governing partial differential equations. In a 2D fixed kernel approach, the approximation $\phi^a(\mathbf{x})$ to the unknown potential $\phi(\mathbf{x})$ is given in discrete form as

$$\phi^a(\mathbf{x}) = \sum_{I=1}^{NS} N_I(\mathbf{x})\hat{\phi}_I \tag{16}$$

and the derivatives of $\phi(\mathbf{x})$ are approximated by

$$\frac{\partial \phi^a}{\partial x}(\mathbf{x}) = \sum_{I=1}^{NS} \frac{\partial N_I}{\partial x}(\mathbf{x})\hat{\phi}_I, \tag{17}$$

$$\frac{\partial^2 \phi^a}{\partial x^2}(\mathbf{x}) = \sum_{I=1}^{NS} \frac{\partial^2 N_I}{\partial x^2}(\mathbf{x})\hat{\phi}_I, \tag{18}$$

where *NS* is the total number of nodes on the semiconductor beam, $\hat{\phi}_I$ is the nodal parameter for node *I*, and $N_I(\mathbf{x})$ is the fixed kernel meshless approximation function of node *I* evaluated at $\mathbf{x}$ (see Refs. 25–27 for details). In a boundary cloud method, the unknown potential $\phi(\mathbf{x})$ and its normal derivative $q(\mathbf{x})$ at a boundary point can be approximated by either a Hermite-type approximation[28] or a varying basis least-squares approximation.[29] The approximation functions are constructed over the boundary nodes without using a mesh. In this paper, we employ a varying basis least-squares approach to approximate the unknown quantities in the BIEs. The discrete form of the varying basis approximation for the unknowns is given by

$$\phi^a(\mathbf{x}) = \sum_{I=1}^{NB} \overline{N}_I(\mathbf{x})\tilde{\phi}_I, \tag{19}$$

$$q^a(\mathbf{x}) = \sum_{I=1}^{NB} \overline{N}_I(\mathbf{x})\tilde{q}_I, \tag{20}$$

where *NB* is the number of boundary points, $\tilde{\phi}_I$ and $\tilde{q}_I$ are the BCM nodal parameters of ϕ and q for node *I*, respectively, and $\overline{N}_I(\mathbf{x})$ is the varying basis approximation function of node *I* (see Ref. 29 for details). After the approximation functions are constructed, the boundary of the structure is discretized into *NC* cells for integration purpose. Each cell contains a certain number of nodes and the number of nodes can vary from cell to cell. Different from an element or a panel in boundary-element methods,[13] the cell can be of any shape or size and the only restriction is that the union of all the cells equal the boundary of the domain.

After the approximation functions are constructed, both the FCM and the BCM use a point collocation technique to discretize the governing equations. In a point collocation approach, the governing equations are satisfied at every node which does not carry a boundary condition, and for nodes with boundary conditions the approximate solution or the derivative of the approximate solution are set to the given Dirichlet and Neumann boundary conditions, respectively. As shown in Fig. 4, we assume that the fixed-fixed semiconductor beam is discretized into *NS* points where the number of boundary points is denoted by *NBS* and the number of interior points is denoted by *NI* ($NI=NS-NBS$). Similarly, the bottom conductor is assumed to be discretized into *NBC* boundary points. The total number of points is denoted by *NT* ($NT=NS+NBC=NI+NBS+NBC$) and the total number of boundary points alone is denoted by *NB* ($NB=NBS+NBC$). We define the *NS* points on the beam as the FCM points, and the *NB* points on the boundaries as the BCM points. Note that the *NBS* points on the boundary of the semiconductor beam are both FCM and BCM points. The FCM substitutes the fixed kernel approximations [Eqs. (16)–(18)] into Eqs. (10) and (13)–(15) to satisfy Poisson's equation or the boundary/interface conditions at the FCM points. The BCM substitutes the varying basis approximations [Eqs. (19) and (20)] into Eqs. (8), (9), (14), and (15) to satisfy the boundary integral equations and the boundary/interface conditions at the BCM points. The discretized Poisson's equation, Eq. (10), for an interior node $\mathbf{x}_i$ is given by

$$\nabla\cdot\left[\varepsilon_s\nabla\left(\sum_{I=1}^{NS} N_I(\mathbf{x}_i)\hat{\phi}_I\right)\right] = -e\left\{p\left[\mathcal{F}_{1/2}\left(\sum_{I=1}^{NS} N_I(\mathbf{x}_i)\hat{\phi}_I\right)\right] - n\left[\mathcal{F}_{1/2}\left(\sum_{I=1}^{NS} N_I(\mathbf{x}_i)\hat{\phi}_I\right)\right] + N_D^+ - N_A^-\right\}, \tag{21}$$

the discretized boundary integral equation, Eq. (9), for a boundary node $\mathbf{x}_i$ is given by

$$\sum_{J=1}^{NB}\left[\alpha(\mathbf{x}_i)\overline{N}_J(\mathbf{x}_i) - \sum_{k=1}^{NC}\int_{\Gamma_k}\overline{N}_J(\mathbf{x}')\frac{\partial G(\mathbf{x}_i,\mathbf{x}')}{\partial n'}d\Gamma(\mathbf{x}')\right]\tilde{\phi}_J = -\sum_{J=1}^{NB}\left[\sum_{k=1}^{NC}\int_{\Gamma_k}\overline{N}_J(\mathbf{x}')G(\mathbf{x}_i,\mathbf{x}')d\Gamma(\mathbf{x}')\right]\tilde{q}_J + \phi_\infty, \tag{22}$$

where Γ_k is the *k*th cell on the boundary. The discretized Dirichlet potential boundary condition, Eq. (13), for an FCM boundary node $\mathbf{x}_i$ is given by

$$\sum_{I=1}^{NS} N_I(\mathbf{x}_i)\hat{\phi}_I = g(\mathbf{x}_i), \tag{23}$$

the discretized Dirichlet potential boundary condition, Eq. (13), for a BCM boundary node $\mathbf{x}_i$ is given by

$$\sum_{J=1}^{NB} \overline{N}_J(\mathbf{x}_i)\tilde{\phi}_J = g(\mathbf{x}_i), \tag{24}$$

the discretized interface conditions, Eqs. (14) and (15), for a boundary node $\mathbf{x}_i$ are given by

$$\sum_{J=1}^{NB} \overline{N}_J(\mathbf{x}_i)\tilde{\phi}_J = \sum_{I=1}^{NS} N_I(\mathbf{x}_i)\hat{\phi}_I, \tag{25}$$

$$\varepsilon_s \sum_{I=1}^{NS} \frac{\partial N_I}{\partial n}(\mathbf{x}_i)\hat{\phi}_I + \varepsilon_d \sum_{J=1}^{NB} \frac{\partial \overline{N}_J}{\partial n}(\mathbf{x}_i)\tilde{q}_J = \sigma(\mathbf{x}_i), \tag{26}$$

and the discretized boundary integral equation, Eq. (8), is given by

$$\sum_{J=1}^{NB}\left[\sum_{k=1}^{NC}\int_{\Gamma_k}\overline{N}_J(\mathbf{x}')d\Gamma(\mathbf{x}')\right]\tilde{q}_J = 0. \tag{27}$$

As shown in Fig. 4, for an interior node of the beam, Eq. (21) is enforced, for a boundary node of the beam with a specified potential boundary condition, Eqs. (22)–(24) are satisfied, for a boundary node on the beam at the dielectric medium interface, Eqs. (22), (25), and (26) are satisfied, for a boundary node on the bottom conductor, Eqs. (22) and (24) are enforced, and finally, Eq. (27) is satisfied separately. It can be easily verfied that Eqs. (21)–(27) give rise to a nonlinear system of $NS+2NB+1$ unknowns and $NS+2NB+1$ equations, which can be rewritten in a general form as

$$R_i(\hat{\phi}_I, \tilde{\phi}_J, \tilde{q}_J, C) = 0 \quad i = 1,2,\ldots,NS+2NB+1,$$
$$I = 1,2,\ldots,NS, \quad J = 1,2,\ldots,NB \tag{28}$$

A Newton's method with line search[31] is used in this paper to solve the nonlinear system given in Eq. (28). The linearized system is given by

$$\begin{bmatrix} \frac{\partial \mathbf{R}}{\partial \hat{\phi}} & \frac{\partial \mathbf{R}}{\partial \tilde{\phi}} & \frac{\partial \mathbf{R}}{\partial \tilde{\mathbf{q}}} & \frac{\partial \mathbf{R}}{\partial \mathbf{C}} \end{bmatrix} \begin{Bmatrix} \delta\hat{\phi} \\ \delta\tilde{\phi} \\ \delta\tilde{\mathbf{q}} \\ \delta\mathbf{C} \end{Bmatrix} = \{-\mathbf{R}\}. \tag{29}$$

In short form, Eq. (29) can be rewritten as

$$[\mathbf{J}]\{\delta\mathbf{u}\} = \{-\mathbf{R}\}, \tag{30}$$

where $\mathbf{J}$ is the Jacobian matrix, $\delta\mathbf{u}$ is the vector of unknown increments, and $\mathbf{R}$ is the residual vector. The nodal parameters $\hat{\phi}$, $\tilde{\phi}$, and $\tilde{\mathbf{q}}$ can be obtained by iteratively solving the nonlinear system. Note that only Eq. (21) is nonlinear. Therefore, only the entries corresponding to Eq. (21) in the Jacobian matrix need to be updated in each iteration. Once the nodal parameters are obtained, the potential ϕ and its normal derivative q can be computed by using Eqs. (16), (19), and (20). The charge distribution in the semiconductor beam structure can be then computed by evaluating the right-hand side of Eq. (10).

Remarks

(1) In the proposed hybrid Poisson/BIE approach, there is no cutoff box and hence no discretization of the exterior dielectric medium is required. Only the boundary of the NEM structures is discretized for the boundary integral equations. As a result, the degrees of freedom of the system are largely reduced.

(2) The boundary integral formulations typically provide accurate results due to the introduction of the fundamental solution, i.e., the Green's function, into the problem formulation. Furthermore, the hybrid approach eliminates the error introduced by the approximated cutoff box boundary condition. The numerical experiments in the paper show that the hybrid BIE/Poisson approach gives a higher accuracy of the solution compared to the conventional approach.

V. HYBRID BIE/POISSON/SCHRÖDINGER APPROACH FOR QUANTUM ELECTROSTATIC ANALYSIS

As the size of the nanoswitch continues to shrink, due to the abrupt change of the potential on the surface of the semiconductor, the semiconductor structure behaves as a quantum well where the carrier concentration at the boundary is much smaller than the concentration in the bulk. To account for the quantum effects in the system, Poisson's equation given in the preceding section is combined with Schrödinger's equation. By solving these two equations self-consistently over the entire semiconductor structure, the potential field and the charge distribution in the system can be determined more accurately. In this section, we extend the hybrid BIE/Poisson approach introduced in Sec. IV to include the solution of Schrödinger's equation. The two dimensional effective mass Schrödinger's equation is given by[32]

$$\hat{H}(\psi_n) = -\frac{\hbar^2}{2m^*}\nabla^2\psi_n + U(V_h, e\phi)\psi_n = E_n\psi_n, \tag{31}$$

where $\hat{H}$ is the Hamiltonian, U is the potential energy, m^* is the effective mass of electrons or holes, ψ_n is the wave function corresponding to the energy level E_n, and V_h is the heterojunction step potential at the side contacts. By solving Schrödinger's equation [Eq. (31)], the energy levels E_n and the corresponding wave functions ψ_n can be obtained for electrons and holes.

The Poisson's equation is coupled with Schrödinger's equation through the quantum electron and hole densities,

$$n_q(\phi) = N_n \sum_n \psi_n^2 \mathcal{F}_{-1/2}\left(\frac{E_F - E_n}{k_B T}\right), \tag{32}$$

$$p_q(\phi) = N_p \sum_n \psi_n^2 \mathcal{F}_{-1/2}\left(\frac{E_n - E_F}{k_B T}\right), \tag{33}$$

where the summation is over all the energy levels and

$$N_n = \frac{1}{\pi}\left(\frac{2m_{nv}^* k_B T}{\hbar^2}\right)^{1/2} \quad N_p = \frac{1}{\pi}\left(\frac{2m_{pv}^* k_B T}{\hbar^2}\right)^{1/2}, \tag{34}$$

where m_{nv}^* and m_{pv}^* are the density-of-state masses of electrons and holes, respectively. Assuming the semiconductor structure to be an ideal quantum well, we enforce the Dirichlet boundary condition for the wave function, $\psi_n = 0$, at the boundary of the semiconductor beam. The discretization of the nanoswitch is shown in Fig. 5. We solve Schrödinger's equation on the same set of points used to solve Poisson's equation (see Sec. IV). The fixed-kernel approximations given in Eqs. (16)–(18) are employed to approximate the unknown wave function ψ_n and its derivatives, i.e.,

$$\psi_n^q(\mathbf{x}) = \sum_{I=1}^{NS} N_I(\mathbf{x})\hat{\psi}_{nI}, \tag{35}$$

$$\nabla^2 \psi_n^a(\mathbf{x}) = \sum_{I=1}^{NS} \nabla^2 N_I(\mathbf{x}) \hat{\psi}_{nI}. \tag{36}$$

Substituting Eqs. (35) and (36) into Eq. (31), Schrödinger's equation can be rewritten in the matrix form

$$\mathbf{H}\hat{\psi}_n = E_n \hat{\psi}_n, \tag{37}$$

where

$$H_{IJ} = -\frac{\hbar^2}{2m^*}\nabla^2 N_J(\mathbf{x}_I) + U[V_h, e\phi(\mathbf{x}_I)]N_J(\mathbf{x}_I)$$
$$I,J = 1,2,\ldots,NS. \tag{38}$$

The discretized eigenvalue problem, Eq. (37), is then solved by using the sparse eigensolver ARPACK (Ref. 33) to obtain the energy levels and the wave functions of electrons and holes. By using Eqs. (32) and (33), the quantum electron and hole densities can be computed.

To obtain a self-consistent solution of Poisson/Schrödinger equations, one needs to iterate between Poisson's and Schrödinger's equations. Since simple underrelaxation scheme usually gives a low convergence rate, in this paper, we employ the predictor-corrector scheme proposed in (Ref. 6). The Poisson's equation is rewritten as

$$\boldsymbol{\nabla} \cdot (\varepsilon_s \boldsymbol{\nabla} \phi) = -e(\tilde{p}_q - \tilde{n}_q + N_D^+ - N_A^-), \tag{39}$$

where the quantum electron and hole densities are replaced by the predictors

$$\tilde{n}_q = N_n \sum_n \psi_n^{(k)2} \mathcal{F}_{-1/2}\left(\frac{E_F - E_n^{(k)} + e(\phi - \phi^{(k)})}{k_B T}\right), \tag{40}$$

$$\tilde{p}_q = N_p \sum_n \psi_n^{(k)2} \mathcal{F}_{-1/2}\left(\frac{E_n^{(k)} - e(\phi - \phi^{(k)}) - E_F}{k_B T}\right), \tag{41}$$

where the superscript k denotes the quantities obtained from the previous iteration. The potential $\phi^{(k+1)}$ is computed by solving the modified Poisson's equation [Eq. (39)]. The wave functions $\psi_n^{(k+1)}$ and the energy levels $E_n^{(k+1)}$ can be obtained by solving Schrödinger's equation using $\phi^{(k+1)}$. Algorithm 1 summarizes the procedure for self-consistent electrostatic analysis of NEM structures by using the hybrid BIE/Poisson/Schrödinger approach.

VI. NUMERICAL EXAMPLES

In this section we perform electrostatic analysis of several nanoswitch devices by using the hybrid approaches. The results obtained by using the hybrid approaches are compared with the results obtained by using the cutoff box approach. Note that, since the focus of this paper is on the development of efficient computational techniques, rather than the investigation of quantum physics in NEM structures, Schrödinger's equation with a simple effective mass approximation is used in all the examples. However, the hybrid approach can be employed for more advanced physical models within the framework of Poisson/Schrödinger equations.

Algorithm 1 Hybrid BIE/Poisson/Schrödinger approach for self-consistent NEMS electrostatic analysis

(1) Discretize the domain of the semiconductor structures and the boundary of the bottom conductors.
(2) Compute the approximation function $N_I(\mathbf{x}_J)$, $I,J=1,2,\ldots,NS$ and its derivatives for the FCM points.
(3) Compute the approximation function $\overline{N}_I(\mathbf{x}_J)$, $I,J=1,2,\ldots,NB$ for the BCM points.
(4) At the initial step $k=0$, set the initial value of the potential to be $\phi^{(0)}=0$
(5) Solve Schrödinger's equation [Eq. (31)] by using $\phi^{(0)}$ to compute $\psi_n^{(0)}$ and $E_n^{(0)}$ for electrons and holes.
(6) Repeat.
(7) Following the procedure described in Sec. IV, solve the coupled BIE/Poisson equations [Eqs. (8), (9), and (39)] using the predictors $\tilde{n}_q(\psi_n^{(k)}, E_n^{(k)})$ and $\tilde{p}_q(\psi_n^{(k)}, E_n^{(k)})$ to obtain potential $\phi^{(k+1)}$.
(8) Solve Schrödinger's equation [Eq. (31)] by using $\phi^{(k+1)}$ to compute $\psi_n^{(k+1)}$ and $E_n^{(k+1)}$ for electrons and holes.
(9) Compute the corrected quantum electron density $n_q^{(k+1)}$ and hole density $p_q^{(k+1)}$ by using Eqs. (32) and (33), respectively.
(10) until $|n_q^{(k+1)} - n_q^{(k)}|$ and $|p_q^{(k+1)} - p_q^{(k)}| <$ error tolerance ε_t

A. Semiclassical analysis

The first example is a nanoswitch containing a 20 nm long and 10 nm wide fixed-fixed silicon beam. The gap between the beam and the bottom conductor is 10 nm. The beam has an N-type doping density of $10^{15}/\text{cm}^3$. The potential at the ends of the beam is specified as 0 V. The applied potential on the bottom conductor is 5 V. The bottom conductor is 40 nm long and 2 nm wide. In this configuration, only the quantization of the electrons needs to be considered and the quantum effect of the holes can be neglected. The system is solved by using both the conventional cutoff box approach and the proposed hybrid BIE/Poisson approach. The discretization of the cutoff box and the potential profile obtained by using the conventional approach is shown in Fig. 6. Figure 7 shows the potential variation in the fixed-fixed silicon beam computed by using the hybrid approach. Note that in the hybrid approach, there is no cutoff box and the exterior dielectric medium is not discretized. Only the boundary of the structure(s) is discretized for the boundary

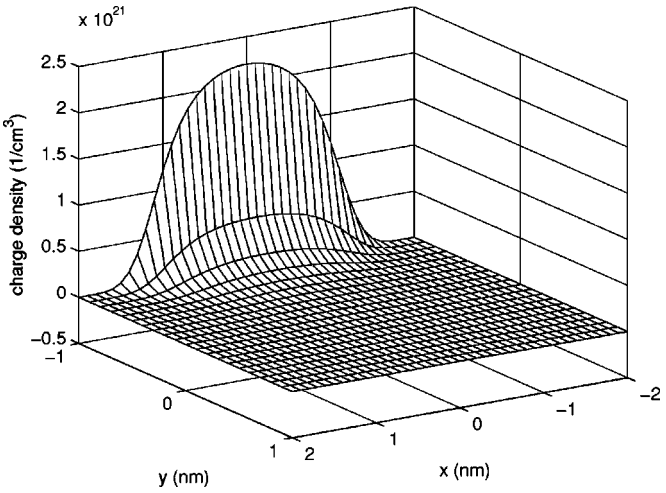

FIG. 11. Charge density profile obtained from the semiclassical analysis.

integral equations. Therefore, the hybrid approach significantly reduces the system size and consequently the computational cost. As shown in Fig. 8, for this example, the system DOFs are reduced by about ten times. Figure 9 shows the CPU time comparison between the two approaches: the hybrid approach is about five times faster compared to the conventional approach. Note that the Jacobian matrix given in Eq. (30) contains dense blocks generated by the boundary integral equations. The computational cost of the hybrid approach can be further reduced by employing acceleration techniques[34] to solve the linear system [Eq. (30)]. On the other hand, the introduction of the Green's function in the BIEs and the elimination of the cutoff box boundary condition improves the accuracy and convergence of the solution. The convergence comparison between the two approaches, shown in Fig. 10, indicates that, by using the BIEs, the hybrid approach achieves a higher accuracy compared to the conventional approach.

B. Quantum-mechanical analysis

The second example is a nanoswitch with a 4 nm $\times$2 nm fixed-fixed silicon beam. The gap between the beam and the bottom conductor is 1 nm. The beam has an *N*-type doping density of $10^{15}/\mathrm{cm}^3$. The potential at the ends of the beam is specified as 0V. The applied potential on the bottom conductor is 5 V. The bottom conductor is 8 nm long and 1 nm wide. The system is solved by using both the semiclassical hybrid BIE/Poisson approach and the quantum-mechanical hybrid BIE/Poisson/Schrödinger approach. Figures 11 and 12 show the charge density profiles obtained from the semiclassical and the quantum-mechanical analysis, respectively. Figures 13 and 14 shows the cross section view (along the width and at the center of the beam) of the charge density and potential profiles, respectively, obtained from the semiclassical and quantum-mechanical analysis. It is clear from the results that when the critical dimension of the NEM structure is just a few nanometers, electron quantum confinement effect is so significant that the quantum-mechanical analysis is necessary.

In the third example, we increase the size of the nanoswitch beam to be 10 nm$\times$10 nm and the gap is 2 nm.

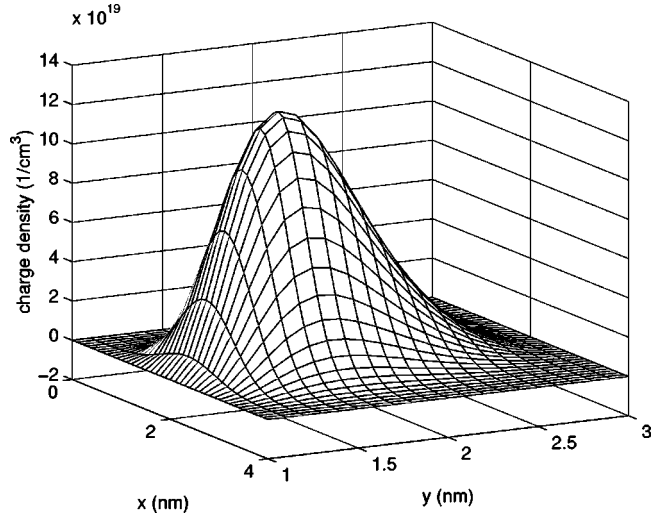

FIG. 12. Charge density profile obtained from the quantum-mechanical analysis.

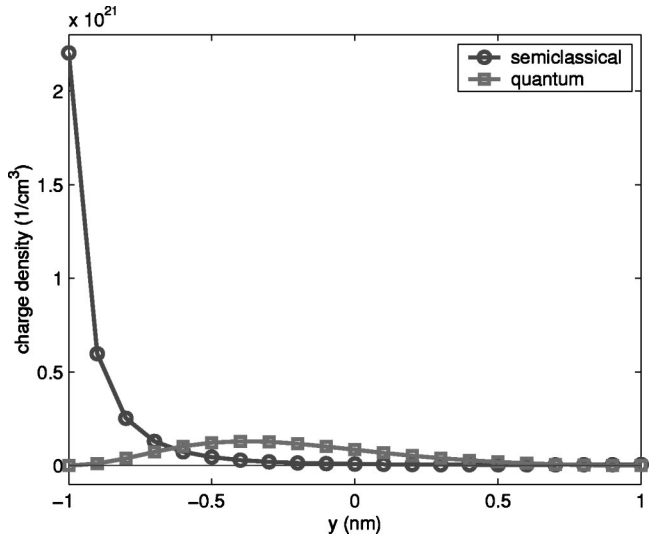

FIG. 13. Comparison of the variation of the charge density along the width obtained from semiclassical and quantum-mechanical analysis.

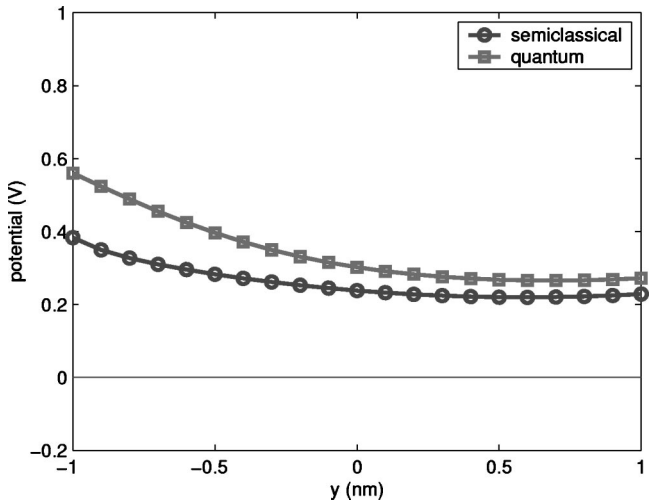

FIG. 14. Comparison of the variation of the potential along the width obtained from semiclassical and quantum-mechanical analysis.

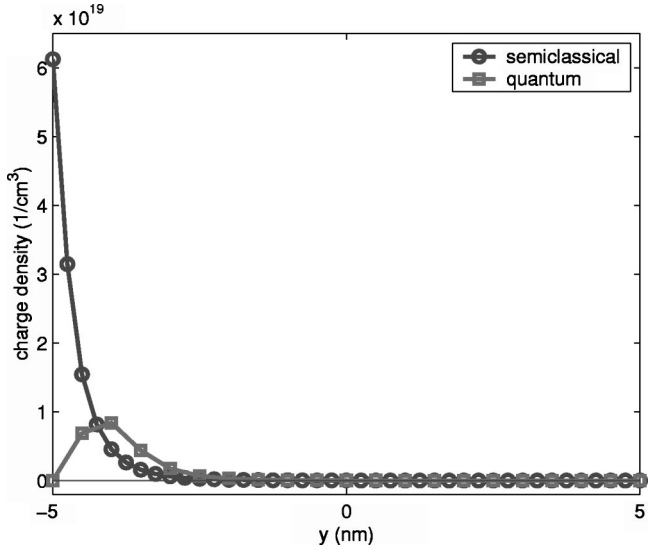

FIG. 15. Comparison of the variation of the charge density along the width obtained from semiclassical and quantum-mechanical analysis.

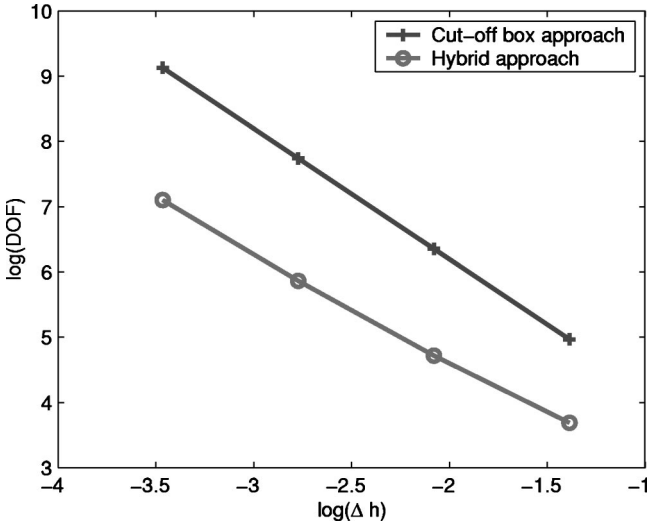

FIG. 17. Degree of freedom comparison between the standard and the hybrid approaches (Δh is the grid spacing).

A potential of 2.5 V is applied on the bottom conductor. The beam is N doped with a density of $10^{15}/\mathrm{cm}^3$. The potential at the ends of the beam is specified as 0 V. Figures 15 and 16 show the cross section view (along the width) of the charge density and the potential profiles at the center of the beam obtained from the semiclassical and quantum-mechanical analysis. In this case, even though the quantum effects are significant only within a 3 nm region from the boundary of the beam, a quantum-mechanical analysis is still necessary to obtain an accurate charge distribution in the beam structure. As shown in Figs. 17 and 18, in this example, the hybrid BIE/Poisson/Schrödinger again reduces the system size (DOFs) by about ten times and gives a higher accuracy compared to the conventional approach.

VII. CONCLUSIONS

The critical dimension in NEMS can vary from several hundred nanometers to just a few nanometers. The semiclassical model can be applied when the critical length of NEM structures is large (typically >30 nm. When the critical dimension of NEM structures is below several tens of nanometers, electron quantum confinement effect can impose a significant effect on the charge distribution in the mechanical components of NEMS and the quantum-mechanical analysis is necessary. In this paper, we propose a hybrid BIE/Poisson approach and a hybrid BIE/Poisson/Schrödinger approach for the semiclassical and quantum-mechanical electrostatic analysis of nanoscale electromechanical systems. We combine the boundary integral equations with the interior Poisson's equation and Schrödinger's equation, along with the meshless finite cloud method and the boundary cloud method, to provide an efficient approach for electrostatic analysis of NEMS. The hybrid approaches significantly reduce the computational cost and provide a higher accuracy of the solution.

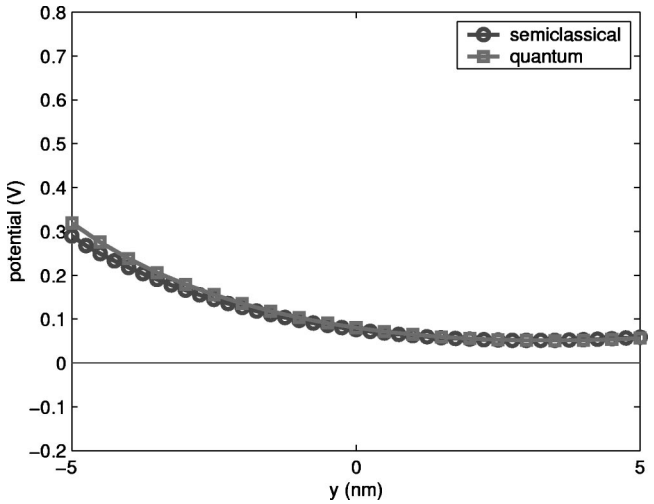

FIG. 16. Comparison of the variation of the potential along the width obtained from semiclassical and quantum-mechanical analysis.

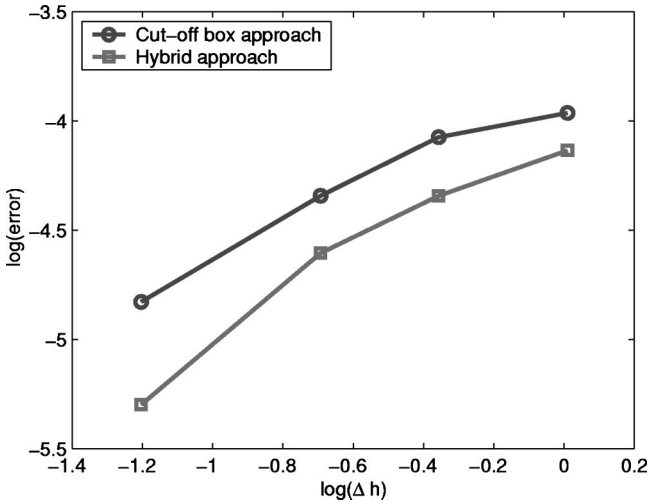

FIG. 18. Convergence comparison between the standard and the hybrid approaches (Δh is the grid spacing). Error is defined the same way as given in the caption of Fig. 10.

ACKNOWLEDGMENTS

This research was supported by the National Science Foundation under Grant No. EEC 0228390. This support is gratefully acknowledged.

[1]M. L. Roukes, Nanoelectromechanical systems, Solid-State Sensor and Actuator Workshop, Hilton Head 2000 pp. 367–376.
[2]F. Stern, Phys. Rev. B **5**, 4891 (1972).
[3]Z. Wu and P. P. Ruden, J. Appl. Phys. **74**, 6234 (1993).
[4]A. Pacelli, IEEE Trans. Electron Devices **44**, 1169 (1997).
[5]S. Lepaul, A. de Lustrac, and F. Bouillault, IEEE Trans. Magn. **32**, 1018 (1996).
[6]A. Trellakis, A. T. Galick, A. Pacelli, and U. Ravaioli, J. Appl. Phys. **81**, 7880 (1997).
[7]Y. Saito, T. Takahashi, and S. Hayano, IEEE Trans. Magn. **23**, 3569 (1987).
[8]M. Ikeuchi, H. Sawami, and H. Niki, IEEE Trans. Microwave Theory Tech. **29**, 234 (1981).
[9]P. P. Silvester, D. A. Lowther, C. J. Carpenter, and E. A. Wyatt, Proc. IEEE **124**, 1267 (1977).
[10]Q. Chen and A. Konrad, IEEE Trans. Magn. **33**, 663 (1997).
[11]M. Gyimesi, J.-S. Wang, and D. F. Ostergaard, Hybrid p-element and trefftz method for capacitance computation, Proc. MSM 2000 pp. 424–428.
[12]D. Givoli, *Numerical Methods for Problems in Infinite Domains* (Elsevier, Amsterdam, 1992).
[13]J. H. Kane, *Boundary Element Analysis in Engineering Continuum Mechanics* (Prentice-Hall, Englewood Cliffs, NJ, 1994).
[14]G. E. Forsythe and W. R. Wasow, *Finite Difference Methods for Partial Differential Equations* (Wiley, New York 1960).
[15]T. J. R. Hughes, *The Finite Element Method* (Prentice-Hall, Englewood Cliffs, NJ, 1987).
[16]M. A. Jaswon and G. T. Symm, *Integral Equation Methods in Potential Theory and Elastostatics* (Academic Press, New York, 1977).
[17]F. Shi, P. Ramesh, and S. Mukherjee, Commun. Numer. Methods Eng. **11**, 691 (1995).
[18]M. Chen, W. Porod, and D. J. Kirkner, J. Appl. Phys. **75**, 2545 (1994).
[19]R. F. Pierret, *Semiconductor Device Fundamentals* (Addison-Wesley, Reading, MA, 1996).
[20]T. Ando, A. Fowler, and S. Stern, Rev. Mod. Phys. **54**, 437 (1982).
[21]J. H. Luscomb, Nanotechnology **4**, 1 (1993).
[22]I. D. Mayergoyz, J. Appl. Phys. **59**, 195 (1986).
[23]H. Kobeissi, F. M. Ghannouchi, and A. Khebir, J. Appl. Phys. **74**, 6186 (1993).
[24]J. D. Jackson, *Classical Electrodynamics*, 3rd ed. (Wiley, New York, 1999).
[25]N. R. Aluru and G. Li, Int. J. Numer. Methods Eng. **50**, 2373 (2001).
[26]X. Jin, G. Li, and N. R. Aluru, CMES: Computer Modeling in Engineering and Sciences **2**, 447 (2001).
[27]X. Jin, G. Li, and N. R. Aluru, Comput. Methods Appl. Mech. Eng. **193**, 1171 (2004).
[28]G. Li and N. R. Aluru, Comput. Methods Appl. Mech. Eng. **191**, 2337 (2002).
[29]G. Li and N. R. Aluru, Eng. Anal. Boundary Elem. **27**, 57 (2003).
[30]T. Belytschko, Y. Krongauz, D. Organ, M. Fleming, and P. Krysl, Comput. Methods Appl. Mech. Eng. **139**, 3 (1996).
[31]M. T. Heath, *Scientific Computing: An Introductory Survey* (McGraw-Hill, New York, 1997).
[32]A. I. M. Rae, *Quantum Mechanics* (Institute of Physics Publishing, Bristol, 1992).
[33]http://www.caam.rice.edu/software/arpack/
[34]V. Shrivastava and N. R. Aluru, Int. J. Numer. Methods Eng. **56**, 239 (2003).